Synthesis and Conformational Analysis of 1′- and 3′-Substituted 2-Deoxy-2-fluoro-D-ribofuranosyl Nucleosides

by **Grigorii G. Sivets**, **Elena N. Kalinichenko**, and **Igor A. Mikhailopulo***

Institute of Bioorganic Chemistry, National Academy of Sciences, Acad. Kuprevicha 5, 220141 Minsk, Belarus (phone/fax: +375-172-67-81-48; e-mail: igor_mikhailo@yahoo.de)

This paper is dedicated to the fond memory of our colleague Dr. *Galina V. Zaitseva*. She will be sorely missed by her colleagues and friends at the Institute of Bioorganic Chemistry.

Convergent syntheses of the 9-(3-X-2,3-dideoxy-2-fluoro-β-D-ribofuranosyl)adenines **5** (X = N_3) and **7** (X = NH_2), as well as of their respective α-anomers **6** and **8**, are described, using methyl 2-azido-5-*O*-benzoyl-2,3-dideoxy-2-fluoro-β-D-ribofuranoside (**4**) as glycosylating agent. Methyl 5-*O*-benzoyl-2,3-dideoxy-2,3-difluoro-β-D-ribofuranoside (**12**) was prepared starting from two precursors, and coupled with silylated N^6-benzoyladenine to afford, after deprotection, 2′,3′-dideoxy-2′,3′-difluoroadenosine (**13**). Condensation of 1-*O*-acetyl-3,5-di-*O*-benzoyl-2-deoxy-2-fluoro-β-D-ribofuranose (**14**) with silylated N^2-palmitoylguanine gave, after chromatographic separation and deacylation, the N^7-β-anomer **17** as the main product, along with 2′-deoxy-2′-fluoroguanosine (**15**) and its N^9-α-anomer **16** in a ratio of *ca.* 42 : 24 : 10. An in-depth conformational analysis of a number of 2,3-dideoxy-2-fluoro-3-X-D-ribofuranosides (X = F, N_3, NH_2, H) as well as of purine and pyrimidine 2-deoxy-2-fluoro-D-ribofuranosyl nucleosides was performed using the PSEUROT (version 6.3) software in combination with NMR studies.

Introduction. – 2′-Deoxy-2-fluoro *ribo*-nucleosides have great potential for the investigation of chemical and/or biochemical problems in which the ribofuranosyl moiety is involved (see, *e.g.*, [1–4]). They constitute a very important family of analogues of natural nucleosides, displaying a wide variety of biological activities (see, *e.g.*, [5–8]), and are constituents of the nucleic-acid-based gene-silencing molecules such as antisense oligodeoxyribonucleic acids (ODNs), ribozymes, and small interfering RNAs (siRNAs) (see, *e.g.*, [9–13]). Two main peculiarities of 2′-deoxy-2-fluoro *ribo*-nucleosides are responsible for the continuous interest in these compounds. Replacement of the 2′-α-OH group (or 2′-α-H-atom of 2′-deoxy nucleosides) by an α-F-atom leads to *i*) significant strengthening of the glycosyl bond [14][15] and *ii*) remarkable conformational changes in the pentofuranose ring [1]. Further, this type of modification of pyrimidine and purine nucleosides was found to result in a remarkable stabilization of the glycosyl bond towards both chemical [14] and enzymatic [15][16] degradation.

A number of synthetic pathways to this family of biologically important nucleosides have been elaborated, following basically three main approaches:

- Convergent synthesis employing suitable derivatives of 2-deoxy-2-fluoro-D-ribofuranose (for a review, see [17]) as glycosylating agents (see, *e.g.*, [18–21] and refs. cit. therein)

© 2007 Verlag Helvetica Chimica Acta AG, Zürich

15222675, 2007, 9, Downloaded from https://onlinelibrary.wiley.com/doi/10.1002/hlca.200790191 by The Scripps Research Institute Kresge Library, Wiley Online Library on [04/01/2023]. See the Terms and Conditions (https://onlinelibrary.wiley.com/terms-and-conditions) on Wiley Online Library for rules of use; OA articles are governed by the applicable Creative Commons License

Shanghai Hongene Exhibit 1028

- Introduction of a 2′-α-F-atom by fluorination of pyrimidine O^2,2′-anhydro-nucleosides [6][14] or by nucleophilic replacement of the 2′-β-OH group of pyrimidine and purine nucleosides with F_3SNEt_2 (DAST) or other fluorinating agents [5][6][22–26] (for a review, see [27])
- Enzymatic transglycosylation of purines using 2′-deoxy-2′-fluoro-uridine as a donor of the sugar moiety [15][16].

During the course of our studies, we have synthesized a number of 3′-deoxy-3-fluoro α,β-D-*ribo*-nucleosides containing diverse (deoxy, azido, amino, and chloro) substituents at the 2′-C-atom [19–21][28–32]. The conformational analysis of this genus of *ribo*-nucleosides was performed with the aid of the PSEUROT (version 6.3) program [33], using the reparameterized [34] *Karplus*-type relation and empirical bond-correction terms [35]. An astonishing conformational uniformity of the pentofuranose rings was revealed, with a dominating population of the *S*-conformation, which was found to be only marginally dependent on both the character of the C(2′)-α-substituent and the anomeric configuration [35]. This behavior could be satisfactorily rationalized by means of the *Brunck–Weinhold* model [36], which invokes maximum antiperiplanar $\sigma-\sigma^*$ stabilization when the donating bond is the least polar one, and the acceptor orbital is at the most polarized bond.

These data prompted us to investigate the conformation of 2′-deoxy-2′-fluoro α,β-D-*ribo*-nucleosides having variable substituents at C(3′) and C(1′). Furthermore, 3′-amino-2′,3′-dideoxy-2′-fluoro-β-D-ribofuranosyl purine nucleosides are of significant interest as constituents of the $N(3') \rightarrow P(5')$ phosphoramidate oligonucleotides [26]; such oligonucleotides, which are complementary to the RNA template region of human telomerase (hTR), have been shown to be effective inhibitors of the enzyme and, consequently, inhibited cancer cell growth *in vitro* [37].

In the present communication, we report the convergent synthesis of *1*) β- and α-configured 9-(3-azido-2,3-dideoxy-2-fluoro-D-ribofuranosyl)adenine, **5** and **6**, respectively, which were transformed into the respective 3′-amino-3′-deoxy nucleosides **7** and **8**; *2*) of 2′,3′-dideoxy-2′,3′-difluoroadenosine (**13**); and *3*) of 2′-deoxy-2′-fluoroguanosine (**15**), its N^9-α-anomer **16**, and of 7-(2-deoxy-2-fluoro-β-D-ribofuranosyl)guanine (**17**) (see *Schemes 1* and *2* below). Further, we performed a detailed conformational analysis of a number of these 2,3-dideoxy-2-fluoro-3-X-D-ribofuranosides (X = H, F, NH_2, N_3) as well as of purine and pyrimidine 2-deoxy-2-fluoro-D-ribofuranosyl nucleosides, the goal being to gain further insight into the role of different stereo-electronic factors on the pseudorotational equilibrium in nucleosides and pentofuranose sugars.

Results and Discussion. – 1. *Synthesis.* The synthesis of methyl 3-azido-5-*O*-benzoyl-2,3-dideoxy-2-fluoro-β-D-ribofuranoside (**4**), the precursor of the target compounds **5**–**8**, was realized in three steps starting from the β-D-xylofuranoside derivative **1** [30], *via* **2** and **3**, in *ca.* 40% combined yield, using conventional methods (*Scheme 1*). Condensation of **4** with persilylated N^6-benzoyladenine in the presence of an excess $SnCl_4$ in anhydrous MeCN under reflux, followed by chromatographic purification, gave a mixture of the anomeric benzoylated nucleosides, along with the starting compound **4** (20%). Debenzoylation of the nucleoside mixture, followed by chromatographic purification, then afforded the pure nucleosides **5** and **6** in yields of 34 and 8%,

15222675, 2007, 9, Downloaded from https://onlinelibrary.wiley.com/doi/10.1002/hlca.200790191 by The Scripps Research Institute Kresge Library, Wiley Online Library on [04/01/2023]. See the Terms and Conditions (https://onlinelibrary.wiley.com/terms-and-conditions) on Wiley Online Library for rules of use; OA articles are governed by the applicable Creative Commons License

Shanghai Hongene Exhibit 1028

Scheme 1

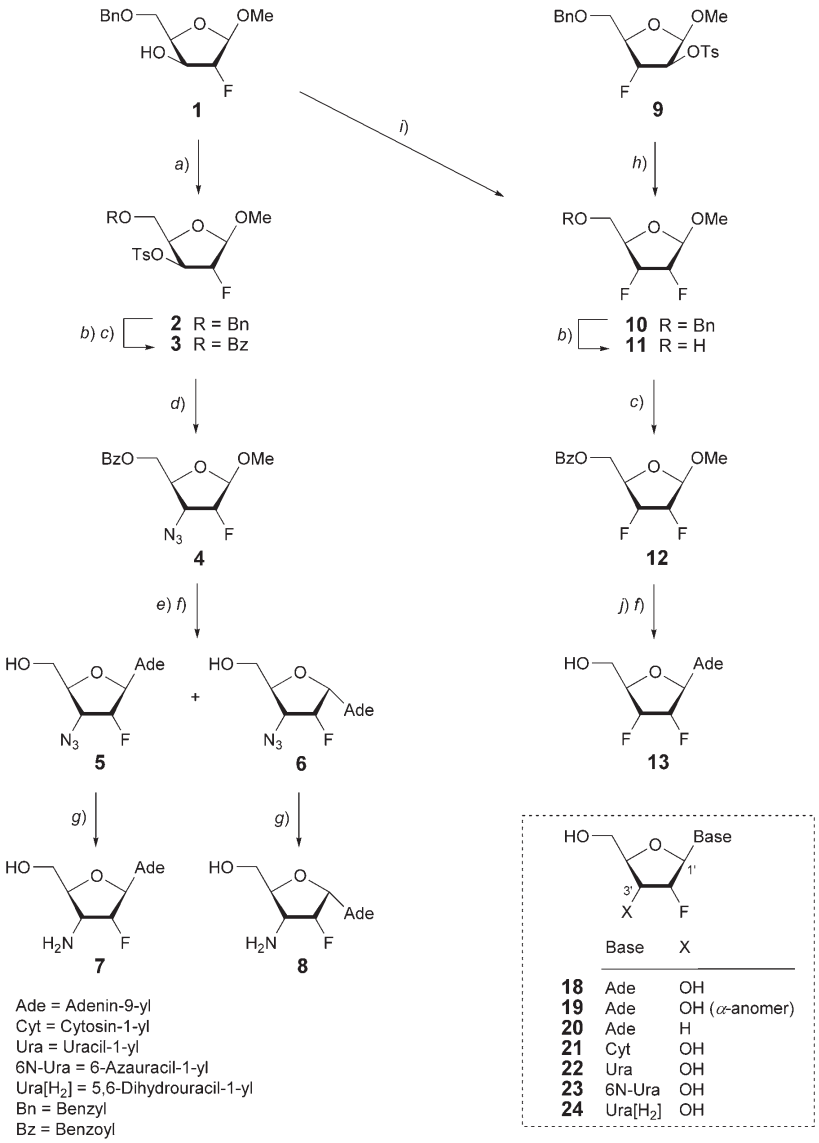

a) TsCl, pyridine, 20°, 72 h; 87%. *b*) [H], 10% Pd/C, EtOH, 20°, 18 h; or 20% $Pd(OH)_2$/C, EtOH, cyclohexene, reflux, 2 h (95% of **11**). *c*) BzCl, pyridine, 20°, 24 h; 85% of **3** (two steps) or 89% of **12** (two steps). *d*) NaN_3, DMSO, 190–195°, 30 min; 51%. *e*) **4**/persilylated N^6-benzoyladenine/$SnCl_4$ 10:19:48, MeCN, reflux, 80 min. *f*) Ammonia-sat. MeOH, 0°, 20°, 18 h; 34% of **5**, 8% of **6** (two steps each). *g*) Ph_3P, pyridine; aq. NH_3; 82% of **7**; 85% of **8**. *h*) CsF, DMSO, 190–195°, 130 min; 32% (based on consumed **9**). *i*) **1**/DAST 10:22, toluene, 20°, 20 h; 30% (based on consumed **1**). *j*) **12**/persilylated N^6-benzoyladenine/$SnCl_4$ 100:175:50, MeCN, reflux, 105 min; 45% (two steps).

15222675, 2007, 9, Downloaded from https://onlinelibrary.wiley.com/doi/10.1002/hlca.200790191 by The Scripps Research Institute Kresge Library, Wiley Online Library on [04/01/2023]. See the Terms and Conditions (https://onlinelibrary.wiley.com/terms-and-conditions) on Wiley Online Library for rules of use; OA articles are governed by the applicable Creative Commons License

Shanghai Hongene Exhibit 1028

respectively. It is noteworthy that no anomerization of **4** was observed, in accord with its low reactivity (see, *e.g.*, [29][30]).

Transformation of the individual azido nucleosides **5** and **6** into the respective 3′-amino-3′-deoxy nucleosides **7** and **8**, respectively, was effected using the *Staudinger* reaction, and the desired compounds were purified by flash chromatography (*Scheme 1*).

Recently, we briefly reported on the synthesis of **13** (see supporting information in [35]), and now provide the full experimental details. Two different routes were tested for the synthesis of the starting difluoride **10**. First, treatment of the xyloside **1** [30] with an excess of DAST in toluene at room temperature proceeded smoothly and furnished, after 20 h, the desired difluoride **10** in 30% yield, based on consumed **1**, 43% of which was recovered. The second route consisted in the nucleophilic displacement of the 2-TsO group of the arabinoside **9** [29][30] upon treatment with CsF in DMSO at 190–195°, which gave, after chromatography, 32% of **10** (based on consumed starting material), along with the initial arabinoside **9** (25%). Attempts to improve the yield of **10**, making use of KF or NaF, failed.

Two-step replacement of the 5-BnO group of **10** by a BzO group afforded **12** in high yield. The latter was allowed to react with persilylated N^6-benzoyladenine, as described above, to afford, after purification, the benzoylated derivative of **13**, together with the starting material **12** (27%) and some impurities. Once again, very low reactivity of the difluorinated methyl glycoside **12** was observed, similar to that of the analogue **4**. Standard deprotection of this fraction, followed by chromatographic purification, finally afforded the desired nucleoside **13** in 45% overall yield.

The synthesis of the target compounds **15**–**17** (*Scheme 2*) was based on condensation of the acetate **14** [19] with silylated N^2-palmitoylguanine in MeCN in the presence of trimethylsilyl triflate (TMS-Tf) under reflux, which gave a complex mixture from which three individual acylated nucleosides were isolated by column chromatography, in 27, 12, and 5% yield, respectively. Standard deacylation of these nucleosides then afforded **17** as the main product, together with the β- and α-anomeric compounds **15** and **16** in good yields as well. The same reaction, but in the presence of an increased amount of TMS-Tf in CH_2Cl_2 at reflux, afforded, after chromatography, the same three nucleosides, in 27%, 19%, and 8% yield, respectively.

Scheme 2

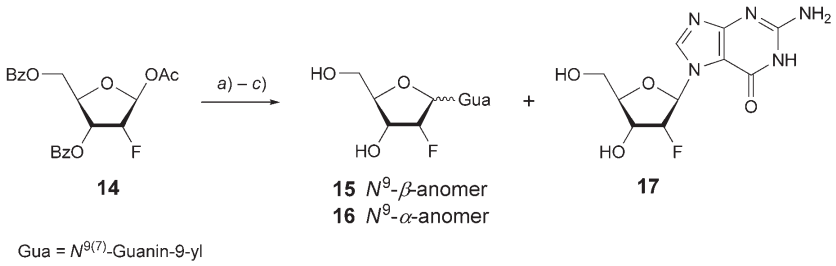

a) **14**/persilylated N^2-palmitoylguanine/TMS-Tf 100:120:155, MeCN, reflux, 3 h [or 100:120:155, CH_2Cl_2, reflux, 5 h]. *b*) Column chromatography (SiO_2). *c*) Ammonia-sat. MeOH, 0°, 20°, 24 h; 10–13% of **15**, 2–5% of **16**, and 22% of **17**.

15222675, 2007, 9, Downloaded from https://onlinelibrary.wiley.com/doi/10.1002/hlca.200790191 by The Scripps Research Institute Kresge Library, Wiley Online Library on [04/01/2023]. See the Terms and Conditions (https://onlinelibrary.wiley.com/terms-and-conditions) on Wiley Online Library for rules of use; OA articles are governed by the applicable Creative Commons License

Shanghai Hongene Exhibit 1028

It is noteworthy that the predominant formation of the N^7-β-nucleoside **17** *vs.* the N^9-β-anomer **15** (ratio *ca.* 2:1) is an exact antithesis to the predominant formation of the N^9-β-anomer in the condensation of silylated N^2-acylguanines with 1-*O*-acetyl-2,5-di-*O*-benzoyl-3-deoxy-3-fluoro-β-D-ribofuranose under similar reaction conditions, as reported before [30]. We have previously shown that the use of an excess of a *Friedel–Crafts* catalyst in the glycosylation reaction allows one to minimize the formation of the N^7-purine isomer (see, *e.g.*, [30][35]). One can hypothesize that the N^7-β-nucleoside **17** is formed under kinetic control, but cannot be isomerized into the thermodynamically more stable N^9-β-isomer **16** owing to *i*) the remarkable stabilization of the glycosyl bond (*vide supra*), or *ii*) the absence of the neighboring 2′-*O*-acyl group, which would facilitate breakdown of the glycosyl bond by intramolecular attack of the C=O function onto the C(1′)-atom.

2. *Spectroscopic Analyses.* The structures of all synthesized compounds were corroborated by in-depth spectroscopic analyses. The assignments of the configurations at the anomeric centers were based upon ^{1}H- and ^{13}C-NMR data (*Tables 1–3*). Thus, the $\beta \rightarrow \alpha$ change of configuration at the anomeric center of each pair of related nucleosides is accompanied by displacement of the H–C(1′) and H–C(4′) resonances to lower field, and a high-field shift of the H–C(2′) resonance (*Table 1*; *cf.* also [30]). Diagnostic for the α-anomeric configurations of the nucleosides **6**, **8**, **16**, and **19** is a long-range coupling of H–C(8) to the 2′-α-F-atom (*Table 2*, last column: J(H,F) = 2.3, 2.3, 3.0, and 2.0 Hz, resp.), and of C(8) to the 2′-α-F-atom (*Table 3*, last column: J(C,F) = 4.9, 3.3, 6.5, and 4.2 Hz, resp.) in their ^{1}H- and ^{13}C-NMR spectra, respectively. These couplings are generally indicative of the physical proximity of the nuclei involved (see, *e.g.*, [19][35] and refs. cit. therein). These couplings were not observed in the corresponding β-anomers **5**, **7**, **13**, **15**, **17**, **18**, and **20**.

A common feature of the above compounds was the very low absolute values of ^3J(C(4′),F), which points to a high preference for the *N*-type pentofuranose-ring conformation. In this conformation, the F–C(2′)–C(3′)–C(4′) fragment is in a clinal (*ca.* 90°) arrangement, consistent with a coupling constant smaller than *ca.* 1.5 Hz.

The CD spectrum of the β-anomer **5** displayed, like that of adenosine [38], a negative long-wavelength *Cotton* effect; in contrast, the 220-nm envelope(s) were missing, and a positive molar ellipticity in the short-wavelength region was observed (*Fig. 1*). As expected, the long-wavelength *Cotton* effect in the CD spectrum of the α-anomer **6** was positive, its maximum being shifted to the far-UV compared to **5**, with an additional shoulder at *ca.* 230 nm and clear trough in the short-wavelength region. The shoulder in the region at 220–240 nm was positive, similar to the 220-nm envelope of α-D-adenosine [38]. Two curves bear a mirror-image relationship. The differences in the shape of the α-anomer **6** *vs.* the β-anomer **5** was attributed to the electronic interaction between the 2′-α-F-atom and the imidazole ring of the purine base in the former.

The CD spectra of the anomeric pair **7** and **8** were found to be approximately mirror images, with a weaker rotational strength in the long-wavelength region compared to **5** and **6**. In contrast to adenosine, the positive 225-nm envelope in the CD spectrum of the β-anomer **7** was absent. However, as in the case of adenosine, the CD curve of the α-anomer **8** showed a clearly resolved, positive *Cotton* effect at 228 nm, which was apparent as a shoulder in the CD spectrum of the α-azide **6**. It is remarkable that both anomers showed clearly resolved negative *Cotton* effects in the short-wavelength

15222675, 2007, 9, Downloaded from https://onlinelibrary.wiley.com/doi/10.1002/hlca.200790191 by The Scripps Research Institute Kresge Library, Wiley Online Library on [04/01/2023]. See the Terms and Conditions (https://onlinelibrary.wiley.com/terms-and-conditions) on Wiley Online Library for rules of use; OA articles are governed by the applicable Creative Commons License

Shanghai Hongene Exhibit 1028

Table 1. [1]*H-NMR Chemical Shifts of Selected Compounds.* Recorded at 500 MHz in CD_3OD, unless noted otherwise; δ in ppm; J in Hz

Cmpd.	H–C(1) or H–C(1′)	H–C(2) or H–C(2′)	H–C(3) or H–C(3′)	H–C(4) or H–C(4′)	H–C(5) or H–C(5′)	H–C(5′) or H–C(5″)	Other signals
4	5.06 (*d*)	5.04 (*dd*)	4.16 (*ddd*)	4.39 (*m*)	4.63 (*dd*)	4.35 (*dd*)	3.31 (*s*, MeO); Bz: 8.08 (*dd*, 2 *o*-H, J = 1.03, 8.21); 7.63 (*tt*, 1 *p*-H); 7.50 (*tt*, 2 H, J = 1.23, 7.75)
4[a])	5.04 (br. *d*)	4.95 (br. *dd*)	4.01 (*ddd*)	4.43–4.47 (*m*)	4.63 (*m*)	4.43–4.47 (*m*)	
5	6.32 (*dd*)	5.76 (*ddd*)	4.66 (*ddd*)	4.22 (*m*)	3.94 (*dd*)	3.77 (*dd*)	8.38 (*s*, H–C(8)); 8.20 (*s*, H–C(2))
6	6.58 (*dd*)	5.52 (*dt*)	4.44 (*dm*)	4.50 (*m*)	3.92 (*dd*)	3.72 (*dd*)	8.30 (*d*, H–C(8)); 8.22 (*s*, H–C(2))
7	6.32 (*dd*)	5.34 (*ddd*)	3.98 (*ddd*)	3.95 (*m*)	3.98 (*dd*)	3.84 (*dd*)	8.43 (*s*, H–C(8)); 8.20 (*s*, H–C(2))
8	6.53 (*dd*)	5.27 (*dt*)	3.88 (*ddd*)	4.31 (*m*)	3.91 (*dd*)	3.74 (*dd*)	8.24 (*d*, H–C(8)); 8.21 (*s*, H–C(2))
12[a])	5.04 (*dd*)	4.92 (*dd*)	5.25 (*dddd*)	4.57 (*ddt*)	4.62 (*dd*)	4.45 (*dd*)	3.33 (*s*, MeO); 8.08, 7.55, 7.45 (3*m*, Bz)
15[b])	6.00 (*dd*)	5.24 (*dt*)	4.36 (*ddd*)	3.92 (*m*)	3.72 (*dd*)	3.56 (*dd*)	7.94 (*s*, H–C(8)); 6.55 (*s*, NH_2); 5.68 (*d*, 3′-OH); 5.14 (*t*, 5′-OH); 10.65 (br. *s*, NH)
16[b])	6.17 (*dd*)	5.13 (*dt*)	4.34 (*ddd*)	4.15 (*m*)	3.65 (*dd*)	3.45 (*dd*)	7.76 (*d*, H–C(8)); 6.49 (*s*, NH_2); 5.81 (*d*, 3′-OH); 4.98 (*t*, 5′-OH); 10.75 (br. *s*, NH)
17[b])	6.32 (*dd*)	5.16 (*ddd*)	4.28 (*ddd*)	3.92 (*m*)	3.78 (*dd*)	3.38 (*dd*)	8.32 (*s*, H–C(8)); 6.12 (*s*, NH_2); 5.66 (*d*, 3′-OH); 5.18 (*t*, 5′-OH); 10.95 (br. *s*, NH)
18	6.29 (*dd*)	5.44 (*ddd*)	4.62 (*ddd*)	4.16 (*m*)	3.94 (*dd*)	3.77 (*dd*)	8.38 (*s*, H–C(8)); 8.20 (*s*, H–C(2))
19	6.52 (*dd*)	5.24 (*dt*)	4.51 (*ddd*)	4.35 (*m*)	3.88 (*dd*)	3.69 (*dd*)	8.32 (*d*, H–C(8)); 8.20 (*s*, H–C(2))
20[b])	6.25 (*d*)	5.61 (*dd*)	2.48 (*dddd*) 2.24 (*ddd*)	4.38 (*m*)	3.74 (*ddd*)	3.57 (*ddd*)	8.35 (*s*, H–C(8)); 8.15 (*s*, H–C(2)); 7.26 (*s*, NH_2); 5.11 (*t*, J(5′,OH) = J(5″,OH) = 5.5; 5′-OH)
21	5.98 (br. *d*)	5.00 (*dd*)	4.30 (*ddd*)	4.08 (*dm*)	4.02 (*dd*)	3.80 (*dd*)	8.28 (*d*, H–C(6)); 6.02 (*d*, H–C(5))
21[b])	5.88 (br. *d*)	4.90 (br. *dd*)	4.12 (*dq*)	3.70–3.92 (*m*)		3.59 (*dd*)	7.92 (*d*, H–C(6)); 5.78 (*d*, H–C(5)); 5.64 (br. *s*, 3′-OH); 5.23 (br. *t*, 5′-OH)
22[b])	5.91 (*dd*)	5.03 (*ddd*)	4.14 (*dm*)	3.87 (*m*)	3.75 (*ddd*)	3.59 (*dt*)	8.10 (*d*, H–C(6)); 5.62 (*d*, H–C(5)); 5.57 (*d*, 3′-OH); 5.16 (*t*, 5′-OH); 11.35 (*s*, NH)
23	6.25 (*d*)	5.16 (*dd*)	4.42 (*ddd*)	3.95 (*m*)	3.82 (*dd*)	3.63 (*dd*)	7.43 (*s*, H–C(5))
24[b])	5.83 (*dd*)	4.95 (*ddd*)	3.99 (*dm*)	3.67 (*dm*)	3.60 (*dd*)	3.45 (*dd*)	3.26 (*ddd*, H–C(6)); 3.39 (*dt*, H–C(5)); 5.40 (br. *s*, 3′-OH); 4.80 (br. *t*, 5′-OH); 10.24 (br. *s*, NH)

[a]) In $CDCl_3$ solution. [b]) In (D_6)DMSO solution.

Shanghai Hongene Exhibit 1028

15222675, 2007, 9, Downloaded from https://onlinelibrary.wiley.com/doi/10.1002/hlca.200790191 by The Scripps Research Institute Kresge Library, Wiley Online Library on [04/01/2023]. See the Terms and Conditions (https://onlinelibrary.wiley.com/terms-and-conditions) on Wiley Online Library for rules of use; OA articles are governed by the applicable Creative Commons License

Table 2. *Selected* $^3J(H,H)$ *and* $J(H,F)$ *Coupling Constants* (in Hz). Recorded at 500 MHz in CD_3OD, unless noted otherwise.

Cmpd.	$J(1,2)$ or $J(1',2')$	$J(2,3)$ or $J(2',3')$	$J(3,4)$ or $J(3',4')$	$J(4,5)$ or $J(4',5')$	$J(4,5')$ or $J(4',5'')$	$J(1,F)$ or $J(1',F)$	$J(3,F)$ or $J(3',F)$	$^2J(2,F)$ or $^2J(2',F)$	Others
4	< 1.0	3.7	8.3	3.7	4.4	10.3	27.6	52.8	$J(5',5'')=12.0$
4[a])	< 1.0	3.7	8.4	n.d.[b])	n.d.	10.1	27.8	53.4	
5	3.1	4.5	6.7	3.0	3.1	16.5	16.5	52.2	$J(5',5'')=12.8$
6	3.5	3.5	8.1	2.4	3.0	18.0	21.7	53.9	$J(5',5'')=12.5$ $J(H-C(8),F)=2.3$
7	< 1.0	4.0	9.4	2.2	2.9	18.0	26.0	52.5	$J(5',5'')=12.2$
8	3.5	3.9	8.2	2.3	3.5	19.6	24.0	54.2	$J(5',5'')=12.3$ $J(8,F)=2.3$
12[a])	< 1.0	3.6	6.8	4.2	4.2	[$J(1,F(2)$ $=9.6$] [$J(2,F(3)$ <2.0]	[$J(3,F(2)$ $=21.0$ [$J(4,F(3)$ $=16.2$]	52.8 51.6	$J(5,5')=11.7$ $J(1,F(3))=1.8$ $J(4,F(2))$ < 1.0
15	2.8	3.6	6.2	2.8	4.0	16.0	18.2	53.0	$J(3',OH)=5.8$ $J(5',OH)$ $=J(5'',OH)=5.5$ $J(5',5'')=13.0$
16	3.9	4.0	7.0	2.5	4.0	18.0	20.0	54.5	$J(3',OH)=6.2$ $J(5',OH)$ $=J(5'',OH)=5.0$ $J(5',5'')=12.5$ $J(8,F)=3.0$
17	2.5	4.2	7.0	2.5	3.5	16.0	20.0	53.0	$J(3',OH)=6.0$ $J(5',OH)$ $=J(5'',OH)=5.5$ $J(5',5'')=12.8$
18	3.4	4.7	5.7	2.2	3.1	15.7	14.8	53.3	$J(5',5'')=12.6$
19	3.9	4.0	6.9	2.2	3.5	16.2	19.2	54.1	$J(5',5'')=12.5$ $J(8,F)=2.0$
20	< 1.0	4.3 [$J(2',3'')$ <1.0]	10.5 [$J(3'',4')$ $=5.6$]	3.3	4.2	18.3	42.1 [$J(3'',F)$ $=20.8$]	51.9	$J(5',5'')=12.1$ $J(3',3'')=14.8$
21	0.9	4.0	8.0	2.0	2.5	17.0	22.5	53.0	$J(C(5),C(6))=7.5$ $J(5',5'')=12.5$
21[c])	0.9	4.2	7.8	n.d.	3.5	18.0	22.8	52.8	$J(C(5),C(6))=7.5$ $J(5',OH)$ $=J(5'',OH)=5.0$ $J(5',5'')=12.5$
22[c])	1.2	3.4	8.7	< 1.5	< 1.9	17.4	20.2	53.2	$J(3',OH)=6.3$ $J(5',OH)$ $=J(5'',OH)=4.6$ $J(5',5'')=12.4$
23	< 1.0	4.4	8.4	2.5	4.9	21.0	23.6	53.4	$J(5',5'')=12.4$
24[c])	3.1	4.9	6.6	2.1	4.0	20.4	17.3	53.6	$J(5',5'')=12.2$

[a]) In $CDCl_3$ solution. [b]) Not determined. [c]) In (D_6)DMSO solution.

15222675, 2007, 9, Downloaded from https://onlinelibrary.wiley.com/doi/10.1002/hlca.200790191 by The Scripps Research Institute Kresge Library, Wiley Online Library on [04/01/2023]. See the Terms and Conditions (https://onlinelibrary.wiley.com/terms-and-conditions) on Wiley Online Library for rules of use; OA articles are governed by the applicable Creative Commons License

Shanghai Hongene Exhibit 1028

Table 3. *Selected* ^{13}*C-NMR Chemical Shifts* (in ppm) *and* J*(C,H) and* J*(C,F) Coupling Constants* (in Hz). Recorded at 125 MHz in CD_3OD, unless noted otherwise.

Cmpd.	C(1) or C(1′) [^2J(C(1′),F)]	C(2) or C(2′) [^2J(C(2′),F)]	C(3) or C(3′) [^2J(C(3′),F)]	C(4) or C(4′)[a])	C(5) or C(5′)	C(2) [J(C(2), H(1′))][b])	C(4) {J(C(4), H(1′))}[c])	C(5)	C(6) [J(C(6), H(1′)][b])	C(8) [J(C(8),F)] {J(C(8), H(1′))}[c])
4[d])	106.9 (*d*) [29.5]	95.6 (*d*) [184.1]	62.0 (*d*) [15.7]	79.5	65.2 (*s*)	–	–	–	–	–
4[e])	105.3 (*d*) [29.2]	95.6 (*d*) [186.1]	60.7 (*d*) [15.8]	78.0	64.0 (*s*)	–	–	–	–	–
5	88.7 (*d*) [33.5]	95.2 (*d*) [190.9]	60.5 (*d*) [15.9]	84.0	61.8 (*s*)	153.8	150.0	121.0	157.4	141.3
6	83.7 (*d*) [15.6]	91.4 (*d*) [194.8]	60.4 (*d*) [15.1]	82.0	60.5 (*s*)	152.8	149.1	118.0	156.0	140.1 [4.9]
7	87.5 (*d*) [23.0]	96.3 (*d*) [193.1]	51.5 (*d*) [17.9]	84.3	60.1 (*s*)	152.7	148.7	119.2	156.5	139.8
8	84.5 (*d*) [15.4]	92.1 (*d*) [191.6]	53.5 (*d*) [17.1]	83.8	60.9 (*s*)	152.6	148.8	118.5	156.1	140.4 [3.3]
15[f])	84.9 (*d*) [32.5]	93.6 (*d*) [186.9]	67.9 (*d*) [16.5]	83.6	60.0	153.7	150.6[g]) {2.0}	116.6[g])	156.6	135.1 {4.0}
16[f])	81.4 (*d*) [15.6]	90.5 (*d*) [193.6]	69.2 (*d*) [16.0]	83.5	60.4	153.7	150.8[g]) {< 1.5}	115.6[g])	156.5	136.2 [6.5] {5.0}
17[f])	87.4 (*d*) [32.7]	94.1 (*d*) [186.8]	67.1 (*d*) [16.0]	83.5	59.6	154.3	160.4[h])	107.2[h])	153.0	141.3 {2.0}
18[f])	85.7 (*d*) [32.7]	93.3 (*d*) [186.9]	68.2 (br. *d*) [18.9]	84.1	60.3 (*s*)	152.4	148.7[h]) {3.8}	119.0[g])	155.8	139.4 {3.8}
19	83.3 (*d*) [15.8]	90.81 (*d*) [194.1]	70.1 (*d*) [16.2]	84.3	60.8	152.5	149.0	118.3	155.9	140.7 [4.2]
20[f])	88.4 (*d*) [35.8]	96.8 (*d*) [177.6]	31.9 (*d*) [20.3]	81.3	61.5	152.6	148.6	119.0	156.0	138.6
21	90.7 (*d*) [34.1]	95.4 (*d*) [186.4]	69.1 (*d*) [16.9]	84.3	60.9	157.9 [< 1.5]	167.7	95.9[i])	142.6[i]) [4.8]	–
21[f])	88.0 (*d*) [33.4]	93.9 (*d*) [185.2]	67.1 (*d*) [15.0]	82.6	59.2	154.8 [2.0]	165.6	93.8	141.0 [2.8]	–
22[f])	87.2 (*d*) [34.2]	93.5 (*d*) [185.7]	67.4 (*d*) [16.2]	83.3	59.4	150.3	163.1	101.6	140.4	–
23	89.7 (*d*) [35.5]	95.4 (*d*) [182.5]	70.8 (*d*) [16.6]	84.3	62.5	158.2	149.5	137.7	–	–
24[f])	86.9 (*d*) [33.6]	92.5 (*d*) [184.6]	69.0 (*d*) [16.0]	82.8	60.8	153.3	170.8	36.8	31.2	–

[a]) In all compounds, the ^3J(C(4′),2(F)) or ^3J(C(4′),2′(F)) values were < 1.5 Hz. [b])[c]) Coupling constants of pyrimidine and purine nucleosides, resp. [d]) MeO Resonance at δ(C) 55.2 (CD_3OD) and 55.5 ($CDCl_3$); benzoyl (Bz) group: 167.61 (C=O); 134.49 (*p*-C); 131.06 (ipso-C); 130.70, 129.62 (*o*- and *m*-C). [e]) In $CDCl_3$. [f]) In (D_6)DMSO. [g]) J(C(5),H(8)) (11.2 and 11.0 Hz) and J(C(4),H(8)) (4.5 and 3.8 Hz) were observed in the ^{1}H-coupled ^{13}C-NMR spectra of **15** and **18**, resp. [h]) J(C(4),H(8)) (13.0 Hz) and the br. *s* of C(5) were observed in the ^{1}H-coupled ^{13}C-NMR spectrum of the N^7-β-isomer **17**. [i]) J(C(5),H(6)) (3.0 Hz), J(C(4),H(5)) (2.0 Hz), and J(C(4),H(6)) (9.0 Hz) were observed in the ^{1}H-coupled ^{13}C-NMR spectrum in CD_3OD.

region (*Fig. 1*). Another unusual example of anomeric pairs having a CD transition of the same sign had been reported earlier by *Ingwall* [38] for the α- and β-pairs of the N^9-D-xylo- and N^9-D-arabinofuranosyl nucleosides of adenine.

15222675, 2007, 9, Downloaded from https://onlinelibrary.wiley.com/doi/10.1002/hlca.200790191 by The Scripps Research Institute Kresge Library, Wiley Online Library on [04/01/2023]. See the Terms and Conditions (https://onlinelibrary.wiley.com/terms-and-conditions) on Wiley Online Library for rules of use; OA articles are governed by the applicable Creative Commons License

Shanghai Hongene Exhibit 1028

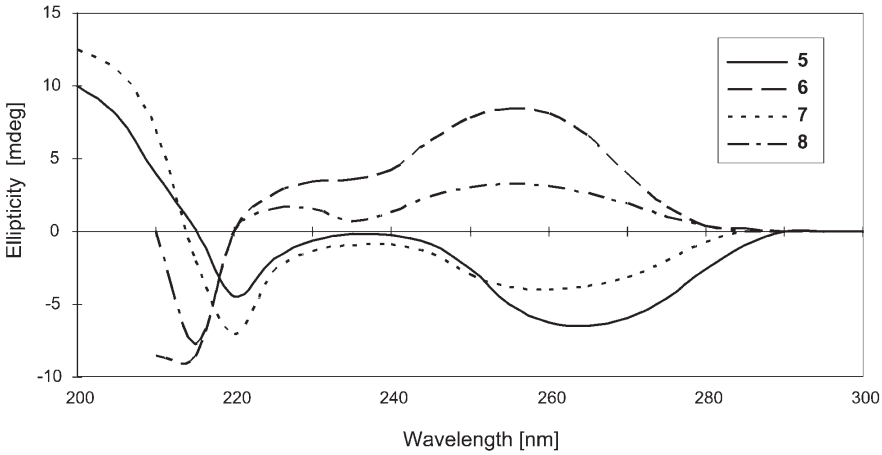

Fig. 1. *Circular dichroism spectra of compounds* **5**–**8** *in EtOH*

The shape of the CD curve of the β-anomer **18** was anomalous, being unexpectedly similar to that of 9-(β-D-xylofuranosyl)adenine [38], with an additional broad positive *Cotton* effect centered at 292 nm (*Fig. 2*). The dependence of the CD spectrum of the nucleosides on the *syn vs. anti* orientation of the heterocyclic base about the glycosyl bond was repeatedly delineated (see, *e.g.*, [38], and refs. cit. therein). To assess the base orientation, we measured the ^3J(C(8),H–C(1′)) and ^3J(C(4),H–C(1′)) coupling constants in the ^{13}C-NMR spectrum of the β-anomer **18** by means of broad-band decoupling of the ^{1}H-NMR resonances (*Table 3*). The value of 3.8 Hz for both coupling constants clearly point to the high rotational mobility of the adenine base about the glycosyl bond [39][40], which is somewhat unexpected, because there are numerous indications for predominant population of the *anti* orientation of purine bases about this bond (compare with the data for some other nucleosides in *Table 3*). It is also noteworthy that the ribofuranose ring of the β-anomer **18** exists in an *N*/S 68:32 pseudorotational equilibrium (*Table 4*), as discussed below. One can suppose that these two factors, *i.e.*, high mobility of the base about the glycosyl bond and the ribofuranose ring, are responsible for the observed anomalous CD curve of **18**.

The CD spectrum of the α-anomer **19** was very similar to that of the α-3′-amino-2′,3′-dideoxy-2′-fluoro nucleoside **8**, the former displaying positive *Cotton* effects more shifted to the far UV and a very stout *Cotton* effect at 215 nm (*Fig. 2*). Further, the CD spectrum of the difluoride **13** was diffuse from 320 to 220 nm, and showed a poorly resolved, negative *Cotton* effect at 268 nm, and another negative CD band at 215 nm (*Fig. 2*).

It was previously discussed that the broad negative and positive *Cotton* effects of the respective β-D- and α-D-pentofuranosyl adenine nucleosides at *ca.* 260 nm contain both the B_{2u} and B_{1u} transitions, together with an $n \rightarrow \pi^*$ transition [38]. The adequate resolution of the B_{2u} and B_{1u} bands in the CD spectra of adenine nucleosides was not observed. However, theoretical considerations and analysis of the shapes of the UV and

15222675, 2007, 9, Downloaded from https://onlinelibrary.wiley.com/doi/10.1002/hlca.200790191 by The Scripps Research Institute Kresge Library, Wiley Online Library on [04/01/2023]. See the Terms and Conditions (https://onlinelibrary.wiley.com/terms-and-conditions) on Wiley Online Library for rules of use; OA articles are governed by the applicable Creative Commons License

Shanghai Hongene Exhibit 1028

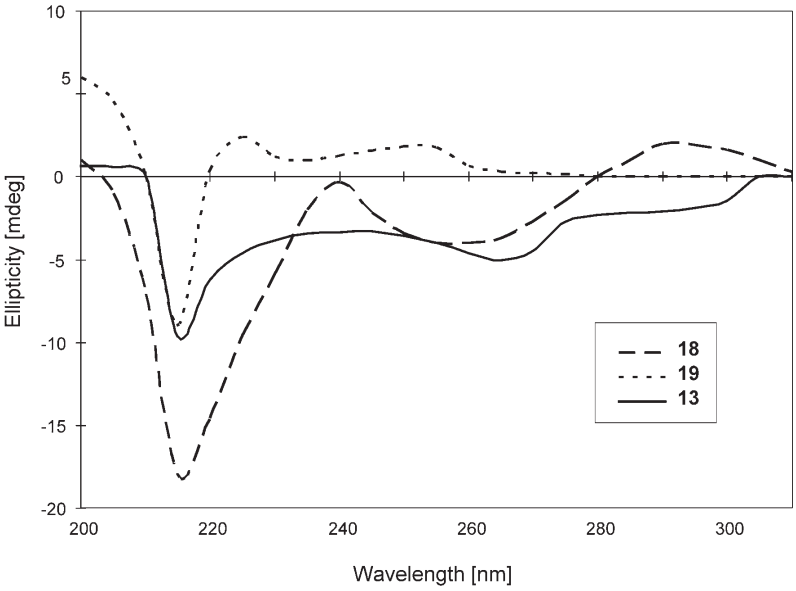

Fig. 2. *Circular dichroism spectra of compounds* **13**, **18**, *and* **19** *in* H_2O

CD envelopes revealed that the *Cotton* effects are controlled by many factors, especially the base orientation about the glycosyl bond and the puckered conformations of the ribofuranose ring. The results of the present work, thus, point to an essential contribution of the electronic character of substituents at C(2′) and C(3′) to the sign and rotational strength of positive or negative *Cotton* effects, especially in the case of the α-anomers.

3. *Conformational Analysis.* The pseudorotational parameters of the compounds investigated are presented in *Table 4*. The conformational analysis of all compounds was performed employing the PSEUROT (version 6.3) program [33], with simultaneous analysis of vicinal H,H and H,F couplings, as described previously [35]. The pseudorotational parameters of compounds **5**–**8** and **15**–**17** were compared with those for the closely related β-anomeric 2′-deoxy-2′-fluoroadenosine (**18**) and its α-anomer **19** [19], as well as the 2′,3′-dideoxy-2′-fluoro derivative **20** [41]. The data for the β-nucleoside **5** were compared with the pseudorotational parameters for the methyl glycoside **4**. Moreover, to gain further insight into the role of the heterocyclic base in the *N*/*S* equilibrium of the 2′-deoxy-2′-fluoro-β-D-pentofuranose ring, conformational analysis of the 2′-deoxy-2′-fluoro pyrimidine nucleosides **21**–**24** was performed (*Table 4*).

All calculations were performed such as to achieving the minimal r.m.s. deviations and $|\Delta J|$ values. Scale factors for ^3J(H,H) and ^3J(H,F) were 1.0 and 0.2, respectively. Moreover, we calculated the geometry-minimized structures for all the compounds studied, using the MM+ and AMBER force fields, and the results were compared with

15222675, 2007, 9, Downloaded from https://onlinelibrary.wiley.com/doi/10.1002/hlca.200790191 by The Scripps Research Institute Kresge Library, Wiley Online Library on [04/01/2023]. See the Terms and Conditions (https://onlinelibrary.wiley.com/terms-and-conditions) on Wiley Online Library for rules of use; OA articles are governed by the applicable Creative Commons License

Shanghai Hongene Exhibit 1028

Table 4. *Pseudorotational Parameters of the Compounds Investigated.* Recorded in CD_3OD, unless noted otherwise. All the PSEUROT data include the $^1H,^1H$ and $^1H,F$ couplings. The P and ν values given in underlined italics were kept fixed during the final minimization.

Cmpd.	P_N [°]	ν_{maxN} [°]	P_S [°]	ν_{maxS} [°]	r.m.s. [Hz]	$\lvert\Delta J\rvert$ [Hz]	S [%]
4	5.5 (^3_2T)	41.3	183.5 (^3_2T)	*28*	0.05	0.10	10
4[a])	11.0 ($^3T_2$)	42.8	*216* (^4_3T)	*40*	0.02	0.03	10
5	−8.0 ($_2T^3$)	*37*	126.6 ($_1E$)	44.6	0.01	0.02	29
6	1.6 (^3_2T)	*44*	133.2 ($_1T^2$)	*44*	0.02	0.07	16
7	25.5 ($^3T_4$)	43.4	*108* (^0_1T)	*44*	0.02	0.04	10
8	−5.8 (^3_2T)	*44*	107.7 (^0_1T)	*44*	0.01	0.03	20
12[a])	−11.8 ($_2T^3$)	41.0	216.0 (^4_3T)	*44*	0.19	0.40	9
[H,F]	−10.3 ($_2T^3$)	39.9	*216* (^4_3T)	*44*	0.16	0.29	7
15[b])	3.8 (^3_2T)	44.7	180.6 (^2_3T)	*36*	0.03	0.08	31
16[b])	4.3 (^3_2T)	37.9	198.9 ($_3E$)	*44*	0.04	0.09	14
17[b])	1.5 (^3_2T)	40.7	126.4 ($_1E$)	*36*	0.03	0.09	24
18	−18.6 ($_2E$)	*37*	125.0 ($_1E$)	43.6	0.02	0.06	32
18[c])	22.2 (^3E)	*44*	210.6 (^4_3T)	*44*	0.03	0.04	39
19	−1.5 (^3_2T)	*44*	127.0 ($_1E$)	*44*	0.01	0.02	32
19[c])	−26.8 ($_2T^1$)	*40*	197.5 ($_3E$)	*44*	0.06	0.09	38
20	4.6 (^3_2T)	36.7	*90* (^0E)	*44*	0.05	0.09	5
21	16.5 (^3E)	38.1	192.8 ($_3E$)	*44*	0.04	0.08	5
21[b])	5.9 (^3_2T)	37.2	201.3 ($_3E$)	*44*	0.04	0.08	5
22[b])	16.9 (^3E)	46.7	136.3 ($_1T^2$)	*44*	0.02	0.07	7
23	17.6 (^3E)	34.9	*198* ($_3E$)	*40*	0.09	0.15	1
24[b])	27.4 ($^3T_4$)	33.1	149.1 (^2_1T)	*36*	0.01	0.03	24

[a]) In $CDCl_3$. [b]) In (D_6)DMSO. [c]) The relevant H,H and H,F coupling constants were taken from the NMR spectra recorded in (D_6)DMSO [19].

those resulting from the PSEUROT calculations. Both force fields afford essentially the same spatial arrangement of the pentofuranose ring for each individual compound, and the outcome of the PSEUROT and molecular-mechanics calculations were mutually consistent as far as the geometry of the most-populated conformer is concerned. Thus, the C(4′)–C(3′)–C(2′)–F torsion angles for the most-populated conformers included in *Table 4* were within 77–83°, which is in fair agreement with the aforementioned ^3J(C(4′),F) value of <1.5 Hz.

In terms of the antiperiplanar effect (APE) proposed by *Brunck* and *Weinhold* [36], and as discussed in detail earlier [35], predominant population of the *N*-type $_2T^3$ conformer (71%) of the ribofuranose ring of the azide **5** results mainly from the strong APE for F–C(2′)–C(3′)–H (torsion angle $\Theta \approx 170°$) and the *N*-driving anomeric effect (ANE) of the base. The APE for N_3–C(3′)–C(2′)–C(1′) ($\Theta \approx 165°$) and the APE for O–C(1′)–C(2′)–H ($\Theta \approx 150°$) also contribute to the *N*-conformer population. The APEs for N_3–C(3′)–C(2′)–H and F–C(2′)–C(3′)–C(4′) ($\Theta \approx 150°$ each), favoring the *S*-form ($_1E$), are weaker in comparison with the strong *N*-driving APEs in the $_2T^3$ conformation.

15222675, 2007, 9, Downloaded from https://onlinelibrary.wiley.com/doi/10.1002/hlca.200790191 by The Scripps Research Institute Kresge Library, Wiley Online Library on [04/01/2023]. See the Terms and Conditions (https://onlinelibrary.wiley.com/terms-and-conditions) on Wiley Online Library for rules of use; OA articles are governed by the applicable Creative Commons License

Shanghai Hongene Exhibit 1028

It is remarkable that the conformational equilibrium of the pentofuranose rings of the azide **5** and the fluorides **15** and **12** are very similar[1]), implying a similar influence of the 3′-OH and 3′-N_3 functions on the *S*/*N* population. On the contrary, the *S*-type conformation (^2E) prevails in 2′,3′-dideoxy-2′,3′-difluoroadenosine (**13**) [35]; interestingly, the most APEs mutually cancel in the *S*- *vs.* *N*-form, except for a strongly *S*-driving APE for F−C(3′)−C(4′)−C(5′), counteracting the *N*-driving ANE. It should be stressed that the anomeric effect of the heterocyclic base diminishes with increasing electronegativity of the 2′-substituent, and in the *β*-D-ribonucleosides it is lower than the ANE in its 2′-deoxy congeners [42] (for a review, see [43]).

The population of the prevailing *N*-type conformers as well as the geometries of the *α*-anomers **6**, **8**, **16**, and **19** are similar. There is a close resemblance of the *N*-type conformers of **6** and **8**, and, as a consequence, of their population. On the contrary, the reason for decreased population of the *N*-type conformer of the adenine *α*-anomer **19** *vs.* the related guanine nucleoside **16** most likely is due to variable strength of numerous related APEs, depending on the geometry of the $_3E$ *vs.* $_1E$ segments of the pseudorotational wheel. On the whole, the *S*/*N* equilibrium of the *β*- and *α*-anomers **18** and **19** appears to be similar, with predominant population of the *N*-type rotamers, *i.e.*, 68% in CD_3OD, and *ca.* 62% in (D_6)DMSO. However, some peculiarities of this equilibrium are notable. The *S*-type conformers of the **18**/**19** pair in each individual solvent are analogous, but the occupied segments of the pseudorotational wheel, $_1E$ in CD_3OD, and $_3E$ in (D_6)DMSO, are rather different. The *N*-type conformers of both anomers in the studied solvents demonstrate remarkable diversity, which, however, is not reflected on the population level.

In the case of the *α*-anomer **6**, the *N*-type (^3_2T) conformation issued from a calculation was found to be more populated (84%) compared to that of the *β*-counterpart **5**. By going from the *β*- to the *α*-anomer, the removal of ANE in the *N*-conformer is compensated by the emerging strong *N*-driving APE for F−C(2′)−C(1′)−H ($\Theta \approx 170°$), far overweighing the *S*-driving ANE of the *S* ($^1T_2$) conformation. In addition, a slight $_1E$ (**5**) → $_1T^2$ (**6**) change of the *S*-type sugar conformer resulted in the clinal arrangement of the 2′-F-atom and the 3′-H-atom, which cannot be compensated by the emerging APE for N_3−C(3′)−C(2′)−H ($\Theta \approx 160°$), leading to a reduced percentage of the latter conformation.

The close similarity of the minor *S*-type conformers of the anomeric pairs **5**/**6**, **7**/**8**, **15**/**16**, and **18**/**19** is remarkable. On the other hand, the *β* → *α* transfer of anomeric configuration results in the decrease of the *S*-type conformation in the case of the **5**/**6** pair (in CD_3OD) and the **15**/**16** pair (in (D_6)DMSO), remains unchanged in the **18**/**19** pair (in both solvents), and is displaced in opposite direction in the **7**/**8** pair (in CD_3OD). The most plausible explanation of such diversity of related anomeric pairs consists in the interplay of subtle differences of APEs and ANEs of the individual conformers. At the same time, differential stabilization by the solvent cannot be excluded.

---

[1]) The MM+ calculation yielded for these three compounds the ^3E conformation, with APEs for F−C(2′)−C(3′)−H ($\Theta \approx 170°$), HO−C(3′)−C(2′)−C(1′) ($\Theta \approx 165°$), and O−C(1′)−C(2′)−H ($\Theta \approx 145°$), resp.

15222675, 2007, 9, Downloaded from https://onlinelibrary.wiley.com/doi/10.1002/hlca.200790191 by The Scripps Research Institute Kresge Library, Wiley Online Library on [04/01/2023]. See the Terms and Conditions (https://onlinelibrary.wiley.com/terms-and-conditions) on Wiley Online Library for rules of use; OA articles are governed by the applicable Creative Commons License

Shanghai Hongene Exhibit 1028

The β-nucleoside **7** exists in the N ($^3T_4$)$\rightleftharpoons S$ (^0_1T) equilibrium, with a strong preference for the former. The strong N drive is due to an APE for F–C(2′)–C(3′)–H ($\Theta \approx 165°$) and an ANE, whereas in the S-type conformation there are no *trans* arrangements between an F-atom and H–C(3′) and C(4′). By going from the β-anomer **7** to its α-counterpart **8**, the geometry of the prevailing N-conformation slightly changes ($^3T_4 \rightarrow {}^3_2T$) and, contrary to the β,α-pair **5/6**, gets less populated. The difference in the S-type population between the α-anomers **6** and **8** may be connected with the more stabilizing APE for F–C(2′)–C(3′)–H in the ^0_1T conformation ($\Theta \approx 160°$) *vs.* that of the $_1T^2$ conformation (a clinal arrangement of 2′-F and 3′-H) as well as by the contribution of an APE for H_2N–C(3′)–C(4′)–C(5′) ($\Theta \approx 160°$).

As mentioned above, 2′,3′-dideoxy-2′,3′-difluoroadenosine (**13**) exists in the N (^3E)$\rightleftharpoons S$ (^2E) equilibrium, with a strong preference (85%) for the latter [35]. Assuming similar strengths of the APE for F–C(2′)–C(3′)–H and APE for F–C(3′)–C(2′)–C(1′) in the N-form on one hand, and of the APE for F–C(3′)–C(2′)–H and APE for F–C(2′)–C(3′)–C(4′) in the S-form on the other hand, we hypothesized that the prevailing S-pseudorotamer results from the interplay between the N-driving ANE and the S-driving APE for F–C(3′)–C(4′)–C(5′). Taking into account that the ANE of the heterocyclic base diminishes with increasing electronegativity of the 2′-substituent [42], one can expect its remarkable weakening in going from β-D-ribonucleosides to their 2′-deoxyfluoro derivatives. The results of the present study, thus, further support this suggestion. Indeed, replacement of the 3′-*ribo* F-atom with OH, N_3, or NH_2 groups resulted in a consecutive decrease of the S-rotamer population, originating from the dramatic drop of electronegativity and, as a consequence, by weakening of the APEs for X–C(3′)–C(2′)–H and X–C(3′)–C(4′)–C(5′) (X = OH, N_3, NH_2). As might be expected, the N-type conformation becomes dominating in the case of 9-(2,3-dideoxy-2-fluoro-β-D-*erythro*-pentofuranosyl)adenine (**20**) (*Table 4*).

The strong preference for the N-type rotamer (90%) of the methyl glycoside **4** compared to the nucleoside **5** is in accord with the stronger anomeric effect of the MeO group *vs.* the adenine base [44]. It is noteworthy that the N (^3_2T)$\rightleftharpoons S$ (^2_3T) equilibrium of **4** was found to be analogous in $CDCl_3$ and in MeOH. Moreover, there is a close resemblance of the pseudorotational parameters of the N/S equilibrium of the methyl β-D-glycosides **4** and **12** in $CDCl_3$ solution (*Table 4*). The dominating population of the N-type rotamers appears to be opposite to predictions based on the conventional gauche effect (GE). Indeed, the GE for F–C(2′)–C(1′)–O(4′) in the N-form should balance the GE for F–C(3′)–C(4′)–O in the S-form, but there remains the strongly S-driving GE for F–C(2′)–C(1′)–OMe, which counteracts the N-driving ANE of the MeO group. We have earlier shown that the GE for F–C(3′)–C(4′)–O is much larger than the ANE for the MeO group [35]; and one can expect a similar relationship between the aforementioned competing GE for F–C(2′)–C(1′)–OMe and the ANE for MeO, displacing the N/S equilibrium to the S-type rotamer.

The dominating population of the N-type conformers of glycosides **4** and **12** is in harmony with the APE proposed by *Brunck* and *Weinhold* [36]. In the case of the difluoride **12**, the APEs for F–C(2′)–C(3′)–H, for H–C(2′)–C(1′)–O, and for F–C(3′)–C(2′)–C(1′) in the N-form balance the APEs for F–C(3′)–C(2′)–H, for H–C(3′)–C(4′)–O, and for F–C(3′)–C(4′)–C(5′) in the S-form, respectively. As a

15222675, 2007, 9, Downloaded from https://onlinelibrary.wiley.com/doi/10.1002/hlca.200790191 by The Scripps Research Institute Kresge Library, Wiley Online Library on [04/01/2023]. See the Terms and Conditions (https://onlinelibrary.wiley.com/terms-and-conditions) on Wiley Online Library for rules of use; OA articles are governed by the applicable Creative Commons License

Shanghai Hongene Exhibit 1028

result, only one weak APE, that for C(3′)–C(2′)–C(1′)–OMe, remains in the *S*-form, and the ANE for the MeO group assumes the predominant role, so that the *N*-form is strongly favored. Similar cancellations are operating in the case of **4**, and the *N*/*S* equilibrium is dominated by the strong *N*-driving ANE for the MeO group.

Consideration of the conformational behavior of a number of compounds studied using the viewpoint of *Brunck* and *Weinhold* on the gauche effect (GE) [36] appears to be satisfactory. We have, however, earlier noted that, in some cases, the calculated pseudorotational equilibrium can be rationalized by the standard model of the GE [44]. For example, the conformational behavior of **13** results from the balancing of all GEs, except for a strongly *S*-driving GE [for F–C(2′)–C(1′)–N(9)][2]), counteracting the weak *N*-driving ANE [36].

Recently, the conformations of the *erythro*- and *threo*-configured diastereoisomers of 1,2-difluorodiphenylethanes and 2,3-difluorosuccinic acids and their derivatives, with the general formula RCHF–CFHR, were investigated and discussed in detail [45]. The predominant population of these molecules with a gauche arrangement of F-atoms (torsion angle *ca.* 60°) was rationalized on the basis of the so-called 'fluorine gauche effect'. It is interesting to note that, in most cases, the gauche arrangement of F-atoms can be rationalized using the viewpoint of *Brunck* and *Weinhold* [36]. There, the relative stabilization of the gauche arrangement of vicinal F-atoms originates from the approximately antiperiplanar orientation of the most electronegative (F, COO^-, *etc.*) and the least electronegative ligand (H, Ar).

The very important role of the electronic nature of the heterocyclic base in terms of the *N*/*S* equilibrium is well-documented (see, *e.g.*, [46][47]; for a review, see [43]). We have also noticed in our previous studies essential differences in the ratio of the *N*/*S* population, depending on the type of substituent at the anomeric C-atom, *e.g.*, MeO *vs.* heterocyclic base [20][35] (see above), or pyrimidine *vs.* purine base [35], as well as on the interplay of stereoelectronic effects of the 2′-deoxy-2′-fluoro-β-D-arabinofuranosyl moiety of nucleosides and heterocyclic base [48][49]. In extension of this work, we studied the role of the electronic structure of the heterocyclic base of 2′-deoxy-2′-fluoro-β-D-ribofuranosyl nucleosides in the *N*/*S* equilibrium.

The conformational behavior of the pentofuranose rings of the adenine nucleosides **5** and **18** (in CD_3OD) and of the regioisomeric guanine nucleosides **15** and **17** (in (D_6)DMSO) is rather similar. The prevailing *N*-type conformation of this group of β-D-nucleosides occupies a rather narrow segment (${}_2T^3 \rightleftharpoons {}_2E$) of the pseudorotational wheel, and the *S*-type ${}_1E$ conformation is populated in compounds **5**, **17**, and **18**. Interestingly, the ${}^3_2T$ conformation is the minor and dominating one in the case of **13** and **20**, respectively. On the other hand, the pentofuranose ring of the pyrimidine nucleosides **21**–**23** displays a strong preference for the *N*-conformation, characterized by a narrow ${}^3E \rightleftharpoons {}^3_2T$ segment of the pseudorotational wheel, quite similar to the aforementioned segment of the *N*-type conformations of purine nucleosides. Note that 2′-deoxy-2′-fluorocytidine (**21**) manifests the same *N*/*S* equilibrium in CD_3OD and (D_6)DMSO solutions.

Reduction of the C(5)=C(6) bond of 2′-deoxy-2′-fluorouridine (**22**) gave rise to nucleoside **24**, with increased population of the *S*-conformation, but retention of its

[2]) MM+ Calculations yielded for the ${}^2E$ conformation a Θ value of *ca.* 78°.

15222675, 2007, 9, Downloaded from https://onlinelibrary.wiley.com/doi/10.1002/hlca.200790191 by The Scripps Research Institute Kresge Library, Wiley Online Library on [04/01/2023]. See the Terms and Conditions (https://onlinelibrary.wiley.com/terms-and-conditions) on Wiley Online Library for rules of use; OA articles are governed by the applicable Creative Commons License

Shanghai Hongene Exhibit 1028

geometry. It appears to be reasonable that the alteration of the pseudorotational equilibrium by going from nucleoside **22** to its hydrogenated derivative **24** results from the change in electronic structure of the base.

Conclusions. – We have described the synthesis of a number of purine 2′-deoxy-2′-fluoro-D-ribofuranosyl nucleosides with variable substituents (N_3, NH_2, F, OH, H) at the 3′-position in the *ribo* [α-C(3′)] configuration. The methyl glycosides **4** and **12**, containing a 2′-α-F-atom, showed very low reactivity, remarkably lower compared to previously studied methyl glycosides with an azido or amino function at this position [29][30].

In order to gain further insight into the role of different stereoelectronic factors in the *N*/*S* equilibrium of the pentofuranose rings, we analyzed the conformational behavior of a number of 2,3-dideoxy-2-fluoro-3-X-D-ribofuranosides (X = F, N_3, NH_2, H), as well as of some purine and pyrimidine 2-deoxy-2-fluoro-D-ribofuranosyl nucleosides, using the PSEUROT (version 6.3) software. It was found that the pentofuranose rings of the purine nucleosides are predominantly in the *N*-type conformations, the degree of population of which is decreased with increasing electronegativity of the 3′-α-substituent (H, 95%; NH_2, 90%; N_3, 71%; OH, 68%; F, 15%). The *N*-type ${}^3E \rightleftharpoons {}^3_2T$ conformations are dominating (> 93%) in the case of pyrimidine 2′-deoxy-2′-fluoro-β-D-ribofuranosyl nucleosides. The observed pseudorotational behavior can be rationalized in terms of the antiperiplanar effect proposed by *Brunck* and *Weinhold* [36].

We are grateful to Prof. *Cornelis Altona* (Leiden University, The Netherlands) for numerous fruitful suggestions and discussions of conformational peculiarities of nucleosides. We are thankful to Dr. *Natalja B. Khripach* (Institute of Bioorganic Chemistry) and *Jarkko Roivainen* (University of Kuopio) for recording NMR spectra, and to Dr. *Nicolai I. Garbuz* (Institute of Bioorganic Chemistry) for recording CD spectra. The authors are indebted to Prof. *Frank Seela* (Universität Osnabrück, Germany) for a sample of 2′-deoxy-2′-fluoro-6-azauridine (**23**). *I. A. M.* thanks the *Technology Development Center* (TEKES) of Finland for partial financial support of this study.

Experimental Part

1. *General. 2′-Deoxy-2′-fluoroadenosine* (**18**) and its α-anomer **19** were prepared as described earlier [19]. *9-(2,3-Dideoxy-2-fluoro-β-*D*-*erythro*-pentofuranosyl)adenine* (**20**) was prepared essentially as described in [41]. *2′-Deoxy-2′-fluorocytidine* (**21**) was prepared according to [50], and its deamination [27] gave *2′-deoxy-2′-fluorouridine* (**22**). Catalytic hydrogenation of **22** (0.25 g, 1.0 mmol) was carried out in water (40 ml) at r.t. and atmospheric pressure for 55 min in the presence of 5% Rh on activated alumina as catalyst (*Fluka*), as reported in [51], to afford *2′-deoxy-2′-fluoro-5,6-dihydrouridine* (**24**) as a viscous oil in quant. yield. *6-Aza-2′-deoxy-2′-fluorouridine* (**23**) was kindly supplied by Prof. *Frank Seela*, Universität Osnabrück, Germany.

Unless noted otherwise, all reactions were carried out at r.t. (20°). For workup, org. solns. were dried over anh. Na_2SO_4 for 4 h. Column chromatography (CC): silica gel *60 H* (70–230 mesh; *Merck*, Darmstadt, Germany), unless otherwise indicated. TLC: aluminum-backed silica gel *60 F_{254}* sheets (*Merck*, Germany); eluents: hexane/AcOEt 3:1 (*A*), $CHCl_3$/MeOH 10:1 (*B*), $CHCl_3$/MeOH 4:1 (*C*), or $CHCl_3$/MeOH/H_2O 40:10:1 (*D*). M.p.: *Boetius* apparatus; uncorrected. UV Spectra: *Carl-Zeiss Second M-400* apparatus; λ_{max} (ε) in nm. $[\alpha]^{20}_D$ Values: *Jusco J-20* spectropolarimeter; concentration in g/l. CD Spectra: *Jasco J-20* spectropolarimeter; λ in nm, $[\Theta]_\lambda$ in deg cm^2 dmol^{-1}. IR Spectra: *Carl-Zeiss UR-20* apparatus; in cm^{-1}. ^{1}H- and ^{13}C-NMR Spectra: *Bruker Avance-500-DRX* spectrometer, at 500.13 and

15222675, 2007, 9, Downloaded from https://onlinelibrary.wiley.com/doi/10.1002/hlca.200790191 by The Scripps Research Institute Kresge Library, Wiley Online Library on [04/01/2023]. See the Terms and Conditions (https://onlinelibrary.wiley.com/terms-and-conditions) on Wiley Online Library for rules of use; OA articles are governed by the applicable Creative Commons License

Shanghai Hongene Exhibit 1028

125.76 MHz, resp., at 300 K; δ in ppm rel. to Me_4Si, J in Hz. All NMR assignments were confirmed by 2D ($^1H,^1H$ and $^1H,^{13}C$) correlation spectroscopy. Solvents employed for NMR spectra were CD_3OD and (D_6)DMSO, unless stated otherwise.

2. *Methyl 3-Azido-5-*O*-benzoyl-2,3-dideoxy-2-fluoro-β-*D*-ribofuranoside* (**4**). 2.1. *Methyl 5-*O*-Benzyl-2,3-dideoxy-2-fluoro-3-*O*-[(4-methylphenyl)sulfonyl]-β-*D*-ribofuranoside* (**2**). Reaction of xyloside **1** (3.5 g, 13.65 mmol) [30] with TsCl (5.0 g, 27.0 mmol) in anh. pyridine (20 ml) for 72 h, followed by purification by CC (SiO_2; 0 → 20% AcOEt in hexane) afforded **2**. Yield: 4.9 g (87%). M.p. 50–52° (Et_2O/hexane). TLC (*A*): R_f 0.42. $[\alpha]^{20}_D = -33.0$ ($c = 1.0$, $CHCl_3$). Anal. calc. for $C_{20}H_{23}FO_6S$ (410.46): C 58.52, H 5.65; found: C 58.41, H 5.69.

2.2. *Methyl 5-*O*-Benzoyl-2,3-dideoxy-2-fluoro-3-*O*-[(4-methylphenyl)sulfonyl]-β-*D*-ribofuranoside* (**3**). Compound **2** (4.9 g, 11.94 mmol) was catalytically hydrogenated in the presence of 10% Pd/C (4.9 g) in EtOH (250 ml), followed by standard benzoylation. Yield: 4.3 g (85%). M.p. 80–82° (Et_2O/hexane). TLC (*A*): R_f 0.36. $[\alpha]^{20}_D = -41.5$ ($c = 1.0$, $CHCl_3$). Anal. calc. for $C_{20}H_{21}FO_7S$ (424.44): C 56.60, H 4.99; found: C 56.70, H 4.87.

2.3. *Conversion to* **4**. To a soln. of **3** (0.81 g, 1.91 mmol) in anh. DMSO (10 ml), NaN_3 (0.6 g, 9.23 mmol) was added, and the mixture was heated at 190–195° (bath temp.) for 30 min, cooled, poured into H_2O (10 ml), and extracted with AcOEt (4 × 40 ml). The combined org. extracts were dried and concentrated, and the residue was subjected to CC (SiO_2; AcOEt/hexane 1:15). Yield: 0.29 g (51%). Viscous oil that slowly crystallized on cooling. M.p. 31–32°. TLC (*A*): R_f 0.64. $[\alpha]^{20}_D = +2.0$ ($c = 1.0$, $CHCl_3$). IR (KBr): 1735 (C=O), 2120 (N_3). Anal. calc. for $C_{13}H_{14}FN_3O_4$ (295.27): C 52.88, H 4.78, N 14.23; found: C 52.91, H 4.69, N 14.29.

3. *3′-Azido-2′,3′-dideoxy-2′-fluoroadenosine* (**5**) *and Its α-Anomer* **6**. A mixture of **4** (0.26 g, 0.88 mmol), $SnCl_4$ (0.49 ml, 4.19 mmol), and the bis(trimethylsilyl) derivative of N^6-benzoyladenine[3]) in anh. MeCN (7.0 ml) was heated at reflux for 80 min. After standard workup, the residue was purified by CC (SiO_2; $CHCl_3$) to afford initial **4** (52 mg, 20%) and the benzoylated derivatives of **5**/**6** as a viscous oil (0.2 g), the latter being directly used in the next step. Thus, debenzoylation in ammonia-sat. MeOH (30 ml) at 0° for 18 h and purification by CC (SiO_2; 0 → 9% MeOH in $CHCl_3$) gave 70 mg (34%) of **5** and 17 mg (8%) of **6**.

Data of **5**. M.p. 184–186° (Et_2O/EtOH). TLC (*B*): R_f 0.37. UV (EtOH): 259 (15,360). $[\alpha]^{20}_D = +2.5$ ($c = 1.0$, EtOH). CD (EtOH): 267 (−6,500), 235 (0), 290 (0). Anal. calc. for $C_{10}H_{11}FN_8O_2$ (294.25): C 40.82, H 3.77, N 38.08 , found: C 40.79, H 3.80, N 37.99.

Data of **6**. M.p. 87–89° (Et_2O/EtOH). TLC (*B*): R_f 0.25. UV (EtOH): 259 (14,300). $[\alpha]^{20}_D = +31.0$ ($c = 1.0$, EtOH). CD (EtOH): 213 (−8,700), 230 (sh), 255 (+8,400), 220 (0), 280 (0). Anal. calc. for $C_{10}H_{11}FN_8O_2$ (294.25): C 40.82, H 3.77, N 38.08; found: C 40.80, H 3.82, N 38.19.

4. *3′-Amino-2′,3′-dideoxy-2′-fluoroadenosine* (**7**) *and Its α-Anomer* **8**. Ph_3P (30 mg, 0.11 mmol) was added to a soln. of **5** (20 mg, 0.068 mmol) in pyridine (0.13 ml), and the mixture was stirred for 4 h. Then, conc. aq. ammonia (1.1 ml) was added, and stirring was continued for 40 h. The mixture was concentrated, H_2O (3 ml) was added to the residue, the mixture was extracted with benzene (2 × 20 ml), and then concentrated *in vacuo*. The residue was purified by CC (SiO_2 (*Woelm*, Germany); $CHCl_3$, $CHCl_3$/MeOH 10:1, and $CHCl_3$/MeOH 4:1) to afford 15 mg (82%) of **7**. In a similar way, starting from the α-anomer **6** (0.07 g, 0.238 mmol), 54 mg (85%) of **8** was obtained.

Data of **7**. Oil. TLC (*C*): R_f 0.13. UV (EtOH): 260 (15,100). CD (EtOH): 220 (−7,000), 260 (−4000), 214 (0), 284 (0). Anal. calc. for $C_{10}H_{13}FN_6O_2$ (268.25): C 44.77, H 4.88, N 31.33; found: C 44.59, H 4.70, N 31.40.

Data of **8**. Oil. TLC (*C*): R_f 0.11. UV (EtOH): 260 (14,900). CD (EtOH): 214 (−7,600), 228 (+1,600), 255 (+3,300), 210 (0), 220 (0), 285 (0). Anal. calc. for $C_{10}H_{13}FN_6O_2$ (268.25): C 44.77, H 4.88, N 31.33; found: C 44.70, H 4.75, N 31.45.

5. *Methyl 5-*O*-Benzyl-2,3-dideoxy-2,3-difluoro-β-*D*-ribofuranoside* (**10**). *Method A*. To a soln. of **9** (1.2 g, 2.92 mmol) [30] in anh. DMSO (35 ml) was added freshly dried CsF (2.9 g, 19.09 mmol), and the reaction mixture was stirred at 195–200° (bath temp.) for 130 min. After cooling to r.t., the mixture was

[3]) Obtained from 0.4 g (1.67 mmol) of N^6-benzoyladenine and an excess of hexamethyldisilazane (HMDS) in the presence of $(NH_4)_2SO_4$ under reflux for 3 h.

15222675, 2007, 9, Downloaded from https://onlinelibrary.wiley.com/doi/10.1002/hlca.200790191 by The Scripps Research Institute Kresge Library, Wiley Online Library on [04/01/2023]. See the Terms and Conditions (https://onlinelibrary.wiley.com/terms-and-conditions) on Wiley Online Library for rules of use; OA articles are governed by the applicable Creative Commons License

Shanghai Hongene Exhibit 1028

poured into H_2O (30 ml) and extracted with AcOEt (4 × 100 ml). The combined org. extracts were dried and concentrated, and the oily residue was subjected to CC (SiO_2; 0 → 33% AcOEt in hexane). Yield: 0.18 g (32%, based on consumed (75%) starting material). Oil. TLC (*A*): R_f 0.74.

Method B. To a soln. of **1** (0.6 g, 2.34 mmol) [30] in anh. toluene (8 ml) was added DAST (0.68 ml, 5.19 mmol), and the mixture was stirred for 20 h. Then, the mixture was poured into 20% aq. NH_4HCO_3 soln. and extracted with CH_2Cl_2 (3 × 100 ml). The combined org. extracts were dried and concentrated. The residue was subjected to CC (SiO_2; 0 → 25% AcOEt in hexane). Yield: 0.103 g (30%, based on consumed (57%) starting material).

6. *Methyl 2,3-Dideoxy-2,3-difluoro-β-*D*-ribofuranoside* (**11**). To a soln. of **10** (0.18 g, 0.7 mmol) in anh. EtOH (4 ml) was added 20% $Pd(OH)_2$/C (0.39 g) and freshly dist. cyclohexene (5 ml), and the mixture was heated at reflux for 2 h. After cooling to r.t., the catalyst was filtered off and washed with EtOH (50 ml), and the combined filtrates were concentrated. The residue was purified by CC (SiO_2; 0 → 33% AcOEt in hexane). Yield: 0.11 g (95%). Oil. TLC (*A*): R_f 0.18.

7. *Methyl 5-*O*-Benzoyl-2,3-dideoxy-2,3-difluoro-β-*D*-ribofuranoside* (**12**). Prepared by standard benzoylation of **11** (0.11 g, 0.66 mmol), followed by CC (SiO_2; 0 → 16% AcOEt in hexane). Yield: 0.16 g (89%). Oily substance. TLC (*A*): R_f 0.71.

8. *2′,3′-Dideoxy-2′,3′-difluoroadenosine* (**13**). A mixture of **12** (0.15 g, 0.55 mmol), $SnCl_4$ (0.32 ml, 2.74 mmol), and the bis(trimethylsilyl) derivative of N^6-benzoyladenine (obtained from 0.23 g (0.96 mmol) of N^6-benzoyladenine)[3]) in anh. MeCN (7.5 ml) was heated at reflux for 105 min. After standard workup, the residue was purified by CC (SiO_2; 0 → 5% MeOH in $CHCl_3$) to afford unreacted **12** (40 mg, 27%) and the benzoylated derivative of **13** (0.15 g, with some impurities) as a viscous oil, which was used in the next step without further purification. Thus, standard debenzoylation of the latter product (25 ml ammonia-sat. MeOH, 0°, 18 h), followed by CC (SiO_2; 0 → 6 % MeOH in $CHCl_3$) gave 50 mg (45%) of **13**. Amorphous powder. TLC (*B*): R_f 0.38. UV (H_2O): 261 (14,700). CD (H_2O): 215 (−9,600), 250 (−3,400), 265 (−5,000), 300 (−1,700), 210 (0). Anal. calc. for $C_{10}H_{11}F_2N_5O_2$ (271.22): C 44.28, H 4.09, N 25.82; found: C 44.20, H 4.12, N 25.84.

9. *Condensation of Trimethylsilylated* N^2*-Palmitoylguanine and 1-*O*-Acetyl-3,5-di-*O*-benzoyl-2-deoxy-2-fluoro-β-*D*-ribofuranose* (**14**). A soln. of the acetate **14** (0.8 g, 2.0 mmol) [19], persilylated N^2-palmitoylguanine [obtained from N^2-palmytoylguanine (0.78 g, 2.4 mmol) in analogy to the method described above[3])], and trimethylsilyl triflate (TMS-Tf; 0.69 mg, 0.56 ml, 3.1 mmol) in anh. MeCN (45 ml) was heated at reflux for 3 h. After standard workup, the residue was purified by CC (SiO_2; 0 → 5% MeOH in $CHCl_3$) to afford the following pure *acylated* nucleosides (in order of elution): the N^7-β-isomer as the main product (0.39 g, 27%), the N^9-β-isomer (0.18 g, 12%), and the N^9-α-isomer (75 mg, 5%). [Condensation of the same reagents, but in a molar ratio of 1:1.7:2.4, in CH_2Cl_2 under reflux for 5 h gave, after standard workup and CC, the above acylated nucleosides in yields of 27, 19, and 8%, resp.]. Finally, standard deacylation of the individual acylated isomers (25 ml ammonia-sat. MeOH, 0°, 24 h) gave the pure, deprotected nucleosides, *i.e.*, *7-(2-deoxy-2-fluoro-β-*D*-ribofuranosyl)guanine* (**17**), and *2′-deoxy-2′-fluoroguanosine* (**15**) and its α-anomer **16**, in yields of 80–85%.

Data of **15**. M.p. 262–264° (H_2O) (lit. m.p. 262–264° (H_2O) [18]). TLC (*D*): R_f 0.38. UV (H_2O): 252 (13,100), 276 (sh, 8,000). Anal. calc. for $C_{10}H_{12}FN_5O_4 \cdot H_2O$ (303.24): C 39.61, H 4.65, N 23.09; found: C 39.71, H 4.60, N 22.97. The ^{1}H- and ^{13}C-NMR data were in fair agreement with those previously published [18][24].

Data of **16**. M.p. 283–285° (MeOH). TLC (*D*): R_f 0.24. UV (H_2O): 253 (14,200), 276 (sh, 8,100). Anal. calc. for $C_{10}H_{12}FN_5O_4$ (285.23): C 42.11, H 4.24, N 24.55; found: C 42.29, H 4.30, N 24.00.

Data of **17**. M.p. > 245° (H_2O; dec.). TLC (*D*): R_f 0.3. UV (H_2O): 217 (17,900), 240 (sh, 5,000), 287 (6,200). Anal. calc. for $C_{10}H_{12}FN_5O_4 \cdot 0.5\ H_2O$ (294.24): C 40.82, H 4.45, N 23.80; found: C 40.90, H 4.50, N 23.70.

15222675, 2007, 9, Downloaded from https://onlinelibrary.wiley.com/doi/10.1002/hlca.200790191 by The Scripps Research Institute Kresge Library, Wiley Online Library on [04/01/2023]. See the Terms and Conditions (https://onlinelibrary.wiley.com/terms-and-conditions) on Wiley Online Library for rules of use; OA articles are governed by the applicable Creative Commons License

Shanghai Hongene Exhibit 1028

REFERENCES

[1] W. Guschlbauer, *Acta Biochim. Pol*. **1996**, *43*, 77.
[2] K. Krawiec, B. Kierdaszuk, E. N. Kalinichenko, E. B. Rubinova, I. A. Mikhailopulo, S. Eriksson, B. Munch-Petersen, D. Shugar, *Nucleosides Nucleotides Nucl. Acids* **2003**, *22*, 153.
[3] H. Ford Jr., F. Dai, L. Mu, M. A. Siddiqui, M. C. Nicklaus, L. Anderson, V. E. Marquez, J. J. Barchi Jr., *Biochemistry* **2000**, *39*, 2581.
[4] L. Mu, S. G. Sarafianos, M. C. Nicklaus, P. Russ, M. A. Siddiqui, H. Ford Jr., H. Mitsuya, R. Le, E. Kodama, C. Meier, T. Knispel, L. Anderson, J. J. Barchi Jr., V. E. Marquez, *Biochemistry* **2000**, *39*, 11205, and refs. cit. therein.
[5] J. L. Clark, J. C. Mason, L. Hollecker, L. J. Stuyver, P. M. Tharnish, T. R. McBrayer, M. J. Otto, P. A. Furman, R. F. Schinazi, K. A. Watanabe, *Bioorg. Med. Chem. Lett.* **2006**, *16*, 1712.
[6] J. Shi, J. Du, T. Ma, K. W. Pankiewicz, S. E. Patterson, P. M. Tharnish, P. R. McBrayer, L. J. Stuyver, M. J. Otto, C. K. Chu, R. F. Schinazi, K. A. Watanabe, *Bioorg. Med. Chem*. **2005**, *13*, 1641, and refs. cit. therein.
[7] M. Tisdale, M. Ellis, K. Klumpp, S. Court, M. Ford, *Antimicrob. Agents Chemother*. **1995**, *39*, 2454.
[8] E. I. Boreko, N. I. Pavlova, G. V. Zaitseva, I. A. Mikhailopulo, *Voprosy Virusologii* (Moscow) **2001**, *46*, 40 (*Chem. Abstr.* **2002**, *137*, 57010).
[9] F. Eckstein, *Biochimie* **2002**, *84*, 841.
[10] Y. Dorsett, T. Tuschl, *Nat. Rev. Drug Discov.* **2004**, *3*, 318.
[11] D. M. Dykxhoorn, J. Liberman, *Annu. Rev. Med*. **2005**, *56*, 401.
[12] N. S. Que-Gewirth, B. A. Sullinger, *Gene Ther*. **2007**, *14*, 283.
[13] J. M. Layzer, A. P. McCaffrey, A. K. Tanner, Z. Huang, M. A. Kay, B. A. Sullenger, *RNA* **2004**, *10*, 766.
[14] J. F. Codington, I. Doerr, D. Van Praag, A. Bendich, J. J. Fox, *J. Am. Chem. Soc.* **1961**, *83*, 5030; J. F. Codington, I. Doerr, J. J. Fox, *J. Org. Chem*. **1964**, *29*, 558.
[15] J. V. Tuttle, M. Tisdale, T. A. Krenitsky, *J. Med. Chem*. **1993**, *36*, 119.
[16] G. V. Zaitseva, A. I. Zinchenko, V. N. Barai, N. I. Pavlova, E. I. Boreko, I. A. Mikhailopulo, *Nucleosides Nucleotides* **1999**, *18*, 687.
[17] K. Dax, M. Albert, J. Ortner, B. J. Paul, *Carbohydr. Res.* **2000**, *327*, 47.
[18] H. J. Thomas, K. N. Tiwari, S. J. Clayton, J. A. Secrist III, J. A. Montgomery, *Nucleosides Nucleotides* **1994**, *13*, 309.
[19] I. A. Mikhailopulo, G. G. Sivets, N. E. Poopeiko, N. B. Khripach, *Carbohydr. Res.* **1995**, *278*, 71.
[20] I. A. Mikhailopulo, G. G. Sivets, *Helv. Chim. Acta* **1999**, *82*, 2052.
[21] G. V. Zaitseva, G. G. Sivets, Z. Kazimierczuk, J. A. Vilpo, I. A. Mikhailopulo, *Bioorg. Med. Chem. Lett.* **1995**, *5*, 2999.
[22] R. Ranganathan, *Tetrahedron Lett*. **1977**, *18*, 1291.
[23] M. Ikehara, H. Miki, *Chem. Pharm. Bull.* **1978**, *26*, 2449; M. Ikehara, J. Imura, *Chem. Pharm. Bull.* **1981**, *29*, 3281.
[24] A. M. Kawasaki, M. D. Casper, S. M. Freier, E. A. Lesnik, M. C. Zounes, L. L. Cummins, C. Gonzalez, P. D. Cook, *J. Med. Chem*. **1993**, *36*, 831.
[25] B. S. Ross, R. H. Springer, K. G. Sprankle, G. Vazquez, *Nucleosides Nucleotides* **1997**, *16*, 1645.
[26] R. G. Schultz, S. M. Gryaznov, *Nucl. Acids Res.* **1996**, *24*, 2966.
[27] K. W. Pankiewicz, *Carbohydr. Res.* **2000**, *327*, 87.
[28] G. Kowollik, P. Langen, E. I. Kvasjuk, I. A. Mikhailopulo, DD 158903, Publ. 1983–02–09; G. W. Saizewa, G. Kowollik, P. Langen, I. A. Mikhailopulo, E. I.Kvasjuk, DD 209197 (Akad. Wissenschaften DDR [DD], Publ. 1984–04–25); E. I. Kvasyuk, G. V. Zaitsewa, L. P. Savochkina, Z. G. Chidgeavadze, R. S. Beabealashvilli, P. Langen, I. A. Mikhailopulo, *Bioorg. Chem. (Moscow)* **1989**, *15*, 781 (*Chem. Abstr*. **1990**, *112*, 3274); G. V. Zaitsewa, E. I. Kvasyuk, N. E. Poopeiko, T. I. Kulak, V. E. Pashinnik, V. I. Tovstenko, L. N. Markovskii, I. A. Mikhailopulo, *Bioorg. Chem. (Moscow)* **1988**, *14*, 1275 (*Chem. Abstr*. **1989**, *111*, 7722).
[29] I. A. Mikhailopulo, G. G. Sivets, T. I. Pricota, N. E. Poopeiko, J. Balzarini, E. De Clercq, *Nucleosides Nucleotides* **1991**, *10*, 1743.

15222675, 2007, 9, Downloaded from https://onlinelibrary.wiley.com/doi/10.1002/hlca.200790191 by The Scripps Research Institute Kresge Library, Wiley Online Library on [04/01/2023]. See the Terms and Conditions (https://onlinelibrary.wiley.com/terms-and-conditions) on Wiley Online Library for rules of use; OA articles are governed by the applicable Creative Commons License

Shanghai Hongene Exhibit 1028

[30] I. A. Mikhailopulo, N. E. Poopeiko, T. I. Pricota, G. G. Sivets, E. I. Kvasyuk, J. Balzarini, E. De Clercq, *J. Med. Chem*. **1991**, *34*, 3195.
[31] I. A. Mikhailopulo, T. I. Pricota, N. E. Poopeiko, T. V. Klenitskaya, N. B. Khripach, *Synthesis* **1993**, 700.
[32] J. E. Van der Boogaart, E. N. Kalinichenko, T. L. Podkopaeva, I. A. Mikhailopulo, C. Altona, *Eur. J. Biochem*. **1994**, *221*, 759; E. N. Kalinichenko, T. L. Podkopaeva, N. E. Poopeiko, M. Kelve, M. Saarma, I. A. Mikhailopulo, J. E. Van der Boogaart, C. Altona, *Recl. Trav. Chim. Pays-Bas* **1995**, *114*, 43.
[33] J. van Wijk, C. A. G. Haasnot, F. A. A. M. de Leeuw, B. D. Huckriede, A. J. A. Westra Hoekzema, C. Altona, 'PSEUROT 6.3', Leiden Institute of Chemistry, Leiden, The Netherlands, 1999.
[34] C. Thibaudeau, J. Plavec, J. Chattopadhyaya, *J. Org. Chem*. **1998**, *63*, 4967.
[35] I. A. Mikhailopulo, T. I. Pricota, G. G. Sivets, C. Altona, *J. Org. Chem*. **2003**, *68*, 5897.
[36] T. K. Brunck, F. J. Weinhold, *J. Am. Chem. Soc*. **1979**, *101*, 1700.
[37] M. Egli, S. M. Gryaznov, *Cell. Mol. Life Sci*. **2000**, *57*, 1440.
[38] J. S. Ingwall, *J. Am. Chem. Soc*. **1972**, *94*, 5487.
[39] D. B. Davies, *Prog. Nucl. Magn. Reson. Spectrosc.* **1978**, *12*, 135.
[40] A. A. Akhrem, I. A. Mikhailopulo, A. F. Abramov, *Org. Magn. Reson*. **1979**, *77*, 7.
[41] P. Herdewijn, R. Pauwels, M. Baba, J. Balzarini, E. De Clercq, *J. Med. Chem*. **1987**, *30*, 2131.
[42] C. Thibaudeau, J. Plavec, J. Chattopadhyaya, *J. Org. Chem*. **1996**, *61*, 266.
[43] C. Thiebaudeau, J. Chattopadhyaya, 'Stereoelectronic Effects in Nucleosides and Nucleotides and Their Structural Implications', Uppsala University Press, Uppsala, Sweden, 1999.
[44] S. Wolfe. *Acc. Chem. Res.* **1972**, *5*, 102.
[45] D. O' Hagan, H. S. Rzepa, M. Schuler, A. M. Z. Slawin, *Beilstein J. Org. Chem*. **2006**, *2*, 19.
[46] H. Rosemeyer, F. Seela, *J. Chem. Soc., Perkin Trans. 2* **1997**, 2341.
[47] F. Seela, G. Becher, H. Rosemeyer, H. Reuter, G. Kastner, I. A. Mikhailopulo, *Helv. Chim. Acta* **1999**, *82*, 105.
[48] I. A. Mikhailopulo, Y. A. Sokolov, J. He, P. Chittepu, H. Rosemeyer, F. Seela, *Nucleosides Nucleotides Nucl. Acids* **2005**, *24*, 701.
[49] F. Seela, X. Peng, H. Li, P. Chittepu, K. I. Shaikh, J. He, Y. He, I. A. Mikhailopulo, *Collect. Czech. Chem. Commun. Symp. Ser.* **2005**, *7*, 1.
[50] R. Mengel, W. Guschlbauer, *Angew. Chem., Int. Ed.* **1978**, *29*, 525.
[51] W. E. Cohn, D. G. Doherty, *J. Am. Chem. Soc*. **1956**, *78*, 2863.

Received April 12, 2007

15222675, 2007, 9, Downloaded from https://onlinelibrary.wiley.com/doi/10.1002/hlca.200790191 by The Scripps Research Institute Kresge Library, Wiley Online Library on [04/01/2023]. See the Terms and Conditions (https://onlinelibrary.wiley.com/terms-and-conditions) on Wiley Online Library for rules of use; OA articles are governed by the applicable Creative Commons License

Shanghai Hongene Exhibit 1028